Toxoplasma acyl-CoA synthetase *Tg*ACS3 is crucial to channel host fatty acids in lipid droplets and for parasite propagation

Sheena Dass[‡], Serena Shunmugam[‡], Sarah Charital[‡], Samuel Duley, Christophe-Sébastien Arnold, Nicholas J. Katris, Pierre Cavaillès, Marie-France Cesbron-Delauw, Yoshiki Yamaryo-Botté[*,§], and Cyrille Y. Botté[*,§]

Apicolipid Team, Institute for Advanced Biosciences, CNRS UMR5309, Université Grenoble Alpes, INSERM U1209, Grenoble, France

Abstract Apicomplexa comprise important pathogenic parasitic protists that heavily depend on lipid acquisition to survive within their human host cells. Lipid synthesis relies on the incorporation of an essential combination of fatty acids (FAs) either generated by a metabolically adaptable de novo synthesis in the parasite or by scavenging from the host cell. The incorporation of FAs into membrane lipids depends on their obligate metabolic activation by specific enzyme groups, acyl-CoA synthetases (ACSs). Each ACS has its own specificity, so it can fulfill specific metabolic functions. Whilst such functionalities have been well studied in other eukaryotic models, their roles and importance in Apicomplexa are currently very limited, especially for *Toxoplasma gondii*. Here, we report the identification of seven putative ACSs encoded by the genome of *T. gondii* (*Tg*ACS), which localize to different sub-cellular compartments of the parasite, suggesting exclusive functions. We show that the perinuclear/cytoplasmic *Tg*ACS3 regulates the replication and growth of *Toxoplasma* tachyzoites. Conditional disruption of *Tg*ACS3 shows that the enzyme is required for parasite propagation and survival, especially under high host nutrient content. Lipidomic analysis of parasites lacking *Tg*ACS3 reveals its role in the activation of host-derived FAs that are used for i) parasite membrane phospholipid and ii) storage triacylglycerol (TAG) syntheses, allowing proper membrane biogenesis of parasite progenies. 🔬Altogether, our results reveal the role of *Tg*ACS3 as the bulk FA activator for membrane biogenesis allowing intracellular division and survival in *T. gondii* tachyzoites, further pointing to the importance of ACS and FA metabolism for the parasite.

Supplementary key words: *Toxoplasma gondii* • apicomplexa • host-parasite metabolic interactions • Lipid metabolism • membrane biogenesis • fatty acid activation • Acyl-CoA synthetase • lipidomic • lipid-fatty acid fluxes

Apicomplexa parasites are a group of unicellular eukaryotes that include obligate intracellular parasites responsible for major human and cattle diseases. These include *Toxoplasma gondii*, *Plasmodium* sp., and *Cryptosporidium parvum*, which are causing agents of the infectious disease toxoplasmosis, malaria, and cryptosporidiosis, respectively. There is currently no fully efficient vaccine, and, depending on the parasite and the related diseases, current treatments can be toxic, losing efficiency and or emergence and fast spreading of resistance amongst parasite populations. There is thus an urgent need to renew our therapeutic arsenal to further push for the eradication of these important diseases. One important step for this is to understand and identify the key metabolic pathways sustaining host-parasite interactions and parasite survival. Metabolic pathways allowing nutrient acquisition, intracellular development, and parasite propagation represent ideal targets for drug development. Lipid synthesis, acquisition, and homeostasis have been shown as one of the key metabolic pathways for parasite survival and pathogenicity (1, 2).

T. gondii is capable of infecting virtually any nucleated cell in mammals and birds, thereby reflecting its metabolic capacities and plasticity in adapting to different nutritional environments. During the intracellular development of *T. gondii*, lipids play an essential role by providing structural building blocks for membrane biogenesis (3, 4), as signaling molecules participating in key events like active invasion and egress
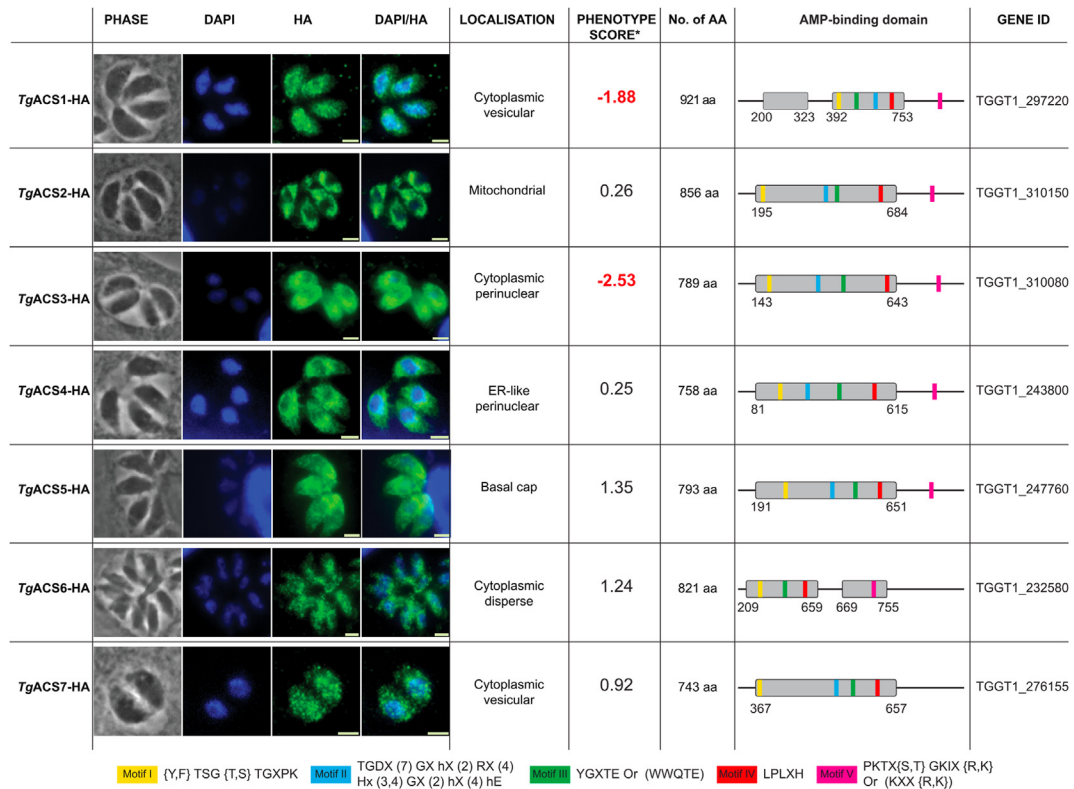
---

through microneme secretion ([5], [6]) and as storage fuels, which plays a critical role to maintain proper intracellular development ([7], [8]). To cope with a continuous need for lipids within the different host cells environments, *T. gondii* has evolved so it harbors three *de novo* synthetic pathways to generate fatty acids (FA), central lipid building blocks: (i) the apicoplast resident prokaryotic type-II fatty acid biosynthesis pathway (FASII) ([4], [9]), (ii) the ER-based FA elongation pathway ([3]) and (iii) the eukaryotic type-I fatty acid synthase present in the cytosol ([9]). Additionally, the parasite is also heavily reliant on acquiring FA directly from their hosts ([7], [8], [10]–[12]). Ongoing research on parasite lipid metabolism suggests that the FA flux derived from both apicoplast FASII ([4], [9]) as well as from direct scavenging from the host ([3], [11]–[13]) are both critical for intracellular parasite viability. Furthermore, in regular growth conditions, most major phospholipid classes making the bulk of *T. gondii* lipid composition are composed of FAs scavenged from the host and FAs made de novo ([4]), forming obligate "patchwork molecules". The metabolic activities of both pathways to acquire and generate FAs are regulated by host nutrient/lipid availability ([13]–[15]). Nutrient/lipid deprivation in the host induces significant upregulations of the apicoplast FASII activity in both *T. gondii* and *P. falciparum* ([12]). On the other hand, lipid scavenging is a constant phenomenon that renders FASII dispensable when the nutrient/lipid content is in excess in the host ([12], [14], [15]).

To cope with this constant flux of FA scavenged from the host, which can be lipotoxic for the parasite, they need to be timely mobilized for bulk phospholipid synthesis and membrane biogenesis, specifically during parasite division ([8], [16], [17]). The parasite accomplishes this by directing excessive FA towards triacylglycerol (TAG) formation which facilitates the biogenesis of lipid droplets (LD). LDs are very conserved organelles present in all eukaryotes and some prokaryotes. They act as the major form of the intracellular store for neutral lipids and constitute an efficient source of energy that can be released as required by the parasite, specifically during their division. FAs need to be metabolically activated to be used by the cell for trafficking, metabolic utilization, or any other cellular function. This key biochemical step is performed by thioesterification of the FA to a Co-Enzyme A (CoA) that is catalyzed by the essential acyl-CoA synthetase (ACS or acyl-CoA ligase) family ([18]). Biochemically, ACSs catalyze a two-step reaction to form fatty acyl-CoA (**Fig. 1**A). The initial step involves the formation of an adenylated intermediate through the hydrolysis of an ATP molecule, thus releasing pyrophosphate ([19]). The ATP-activated enzyme then binds to the carboxyl group of an incoming free FA (FFA) moiety through an acyl bond to the phosphoryl group of AMP. The final fatty acyl-CoA product is formed after the transfer of the fatty acyl group to the sulfhydryl group of coenzyme A, thereby releasing AMP ([19]).

The phylum apicomplexa is actively engaged in FA metabolism, and hence a putatively critical role of ACSs for parasite survival is highly expected. Any putative ACS candidate encoded in the Apicomplexa genome can theoretically activate FAs derived from both de novo synthetic machinery and/or from the host. Such importance and expected functions are supported by the existence of ACS-encoding genes in the genome of Cryptosporidium and Theileria, which lack the de novo fatty acid biosynthetic machinery ([9]). *Cryptosporidium parvum* has been reported to have three AMP-binding domains containing long-chain fatty acid CoA ligases out of which two CpACS1 and CpACS2 have been biochemically characterized as functional ACSs ([20]). *Plasmodium falciparum* on the other hand has a large family of ACSs encoded by 13 genes (PfACS1a-PfACS12) ([21]). They also describe ACSs as the only family of metabolic enzymes that are encoded by genes expanded into the sub-telomeric region, which usually harbors parasite virulence genes ([21]). Drugs specific to ACSs in C. parvum and P. falciparum have shown potent parasite-killing activity, thereby hinting that this enzymatic reaction is a potential Achilles heel for apicomplexans ([22], [23]). Almost nothing is currently known on the function of ACSs in *T. gondii*.

Here, we confirm that the seven genes encoding for seven enzymes we previously identified and classified as putative acyl-CoA synthases, *TgACS* in *Toxoplasma gondii* ([22]), are endogenously expressed by the parasite, and have different localizations, suggesting non-redundant roles ([22]). One of these candidates ACS, *TgACS1*, whose phenotypic score initially suggested it was not important for parasite growth. However, we further showed that the protein's function becomes critical under specific physiological conditions in the host. We reveal that it actually activates FA for their mobilization and use by a peroxisomal-like pathway to provide energy to the parasite under a poor/deleterious host nutritional environment, notably during the tachyzoites extracellular stages. This indicates that the role of such enzymes might be directly linked to the capacity of the parasite to have a strong metabolic plasticity upon host nutritional conditions that strongly govern the metabolic pathways chosen by the parasite ([1], [2], [8], [14], [22], [24]–[26]). The function and potential nutrient-dependent roles of the other ACSs in *T. gondii* are still unknown. Here, we reveal the essential function of another ACS candidate, *TgACS3* ([19]).

Downregulation of *TgACS3*, via a Tet-off-based inducible KD parasite line, revealed that the protein is critical for tachyzoite intracellular development. Cellular characterization shows that *TgACS3* is required to maintain intracellular propagation of *T. gondii* tachyzoites, especially under high host nutrient environments. Lipidomic and fluxomic analyses further determined that the disruption of *TgACS3* significantly reduces the parasite lipid content, phospholipid content, and concomitantly accumulates host FA within the

	PHASE	DAPI	HA	DAPI/HA	LOCALISATION	PHENOTYPE SCORE*	No. of AA	AMP-binding domain	GENE ID
*Tg*ACS1-HA					Cytoplasmic vesicular	**-1.88**	921 aa	200 323 392 753	TGGT1_297220
*Tg*ACS2-HA					Mitochondrial	0.26	856 aa	195 684	TGGT1_310150
*Tg*ACS3-HA					Cytoplasmic perinuclear	**-2.53**	789 aa	143 643	TGGT1_310080
*Tg*ACS4-HA					ER-like perinuclear	0.25	758 aa	81 615	TGGT1_243800
*Tg*ACS5-HA					Basal cap	1.35	793 aa	191 651	TGGT1_247760
*Tg*ACS6-HA					Cytoplasmic disperse	1.24	821 aa	209 659 669 755	TGGT1_232580
*Tg*ACS7-HA					Cytoplasmic vesicular	0.92	743 aa	367 657	TGGT1_276155

Motif I {Y,F} TSG {T,S} TGXPK   Motif II TGDX (7) GX hX (2) RX (4) Hx (3,4) GX (2) hX (4) hE   Motif III YGXTE Or (WWQTE)   Motif IV LPLXH   Motif V PKTX{S,T} GKIX {R,K} Or (KXX {R,K})

Fig. 1. Identification of seven acyl CoA synthetase in *T. gondii* and their cellular localizations. Immunofluorescence of *Tg*ACS1-7 with their respective parasite cellular localization, phenotype score (with the most essential in red), amino acid size, AMP-binding domain location and gene ID. The motif in the AMP-binding domain with their respective amino acid sequences. All scale bars = 2 μm. (this image of *Tg*ACS2 was taken with the *Tg*ACS2-iKD parasite line).

parasite. Together, our data reveal that *Tg*ACS3 is responsible for channeling the constant flux of host FA to generate the bulk of phospholipid for parasite membrane biogenesis, hence maintaining tachyzoite division and survival.

MATERIALS AND METHODS

T. gondii strains and cultures

The parasite-host cells human foreskin fibroblasts (HFF) were cultured using Dulbecco's Modified Eagle's Medium (DMEM, Gibco) supplemented with 10% fetal bovine serum (FBS, Gibco), 2 mM glutamine (Gibco), and 25 μg/ml gentamicin (Gibco) at 37°C and 5% $CO2$. *T.gondii* tachyzoite parental strains RH-ΔKu80 TATi, RH-ΔKu80 as well as the mutant strains were cultured by serial passage within their host HFF using DMEM supplemented with 1% fetal bovine serum (FBS, Gibco), 2 mM glutamine (Gibco) and 25 μg/ml gentamicin (Gibco) at 37°C and 5% $CO2$.

Generation of an inducible knockdown line for Tg*ACS3.* For generation of an inducible knockdown parasite line for the gene *Tg*ACS3, plasmid pPR2-DHFR (27) was used. For homologous recombination in RH-ΔKu80 TATi strain, two separate homology flanks/regions were chosen. The 5′ flank was amplified 1,298 bp upstream of the *Tg*ACS3 start codon using the primers in Table 1. The PCR product was ligated to PacI and NdeI digested vector pPR2 using NEB assembly

reaction. Next, the 3′ flank was amplified as a 1,263 bp fragment beginning at the start codon of *Tg*ACS3 with the primers in Table 1. The 3′ homology flank was annealed to XmaI and NotI digested pPR-HA3-DHFR vector that already contained the *Tg*ACS3 5′ flank. The final cloned vector positions the start codon of *Tg*ACS3 downstream of the ATc-regulatable t7s4 promoter and a 3xHA tag.

The resulting vector was linearized with NotI and transfected into TATiΔku80 parasites. Parasites were selected with the drug pyrimethamine and cloned out by limiting dilution. Screening of parasite clones *Tg*ACS3-iKD where the t7s4 promoter had successfully replaced the native *Tg*ACS3 promoter, was done using the primers in Table 1 in the combinations described in supplementary figures (supplemental Fig. S2A). All PCRs were performed with TaKara Primestar Max polymerase. The knockdown of *Tg*ACS3 was induced with 0.5 μg ml −1 of anhydrotetracycline (ATc).

Immunofluorescence assay

Primary antibodies anti-HA (Rat, Roche), anti-IMC1, and anti-SAG1 were used at dilutions 1:500, 1:1000, and 1:1000 respectively. Secondary Alexa Fluor 488- and 546-conjugated anti-mouse, anti-rat, and anti-rabbit antibodies (Life Technologies) were used at 1/2500. For the immunofluorescence assay (IFA) parasites were grown on confluent HFF on coverslips and fixed in PBS containing 2.5% paraformaldehyde (PFA) for 15 min at room temperature (RT). Samples were permeabilized with 0.25% Triton X-100 in PBS for 10 min at RT prior to blocking in PBS containing 3% BSA and subsequent incubation with primary antibodies then secondary

TgACS Gene ID	Primers (Gene specific sequence underlined)	Molecular system used
*Tg*ACS3 (TGGT1_310080)	5′ flank Fw: GGGCGCGCCGGATCCTTAATTAATCGCTGCGATGTCGATCGTTTTC 5′ flank Rw: CGCCATGCATGGCCGGCCCATATGGCGACTACGAAAGACAAACGCC 3′ flank Fw: TGTTCCAGATTATGCCTTACCCGGGATGGCACTCCAGTACGCCTACC 3′ flank Rw: TGGAGCTCCACCGCGGTGGCGGCCGCCTGCTTCGAGGAGAATGGCTTTC SD01: CGATGACCTGTGTCGACCTGT SD02: TCTTCTTTGAGGGAAGAGGAAACG SD03: GGTACCGAGCTCGACTTTCAC	TATI-Tet off
TgACS1 (TGGT1_297220)	Fw: TACTTCCAATCCAATTTAATGCAGCCTGGGGATGCCGATCAACT Rw: TCCTCCACTTCCAATTTTAGCCAGCTTTGCCTGCAGCGC	pLIC HA tagging
TgACS2 (TGGT1_310150)	Fw: TACTTCCAATCCAATTTAATGCGCGCTCGGCGTTGAGTT Rw: TCCTCCACTTCCAATTTTAGCCGACCACCACGACCGCA	pLIC HA tagging
TgACS4 (TGGT1_243800)	Fw: TACTTCCAATCCAATTTAATGCCTTGCTTGGTGGCCATCATCG Rw: TCCTCCACTTCCAATTTTAGCAATCGCCTTCGCTCTCTCCG	pLIC HA tagging
TgACS5 (TGGT1_247760)	Fw: TACTTCCAATCCAATTTAATGCCCTCGGATCATCGACCGAGC Rw: TCCTCCACTTCCAATTTTAGCATTGGCAGGATGGTGCCGT	pLIC HA tagging
TgACS6 (TGGT1_232580)	Fw: TACTTCCAATCCAATTTAATGCGAAGATGAGATGACCGGGC Rw: TCCTCCACTTCCAATTTTAGCCTTATCTTCGACGTCCTTTACAG	pLIC HA tagging
TgACS7 (TGGT1_276155)	Fw: TACTTCCAATCCAATTTAATGCGAAGCAGGCGAACCTGGA Rw: TCCTCCACTTCCAATTTTAGCGTCGTCGTTCTTCAAAAGTTCG	pLIC HA tagging

antibodies diluted in the blocking solution. Labeled parasites were stained with Hoechst (1/10,000, Life technologies) for 20 min and then washed three times in PBS before final mounting of the coverslips on a glass slide using fluorogel. The fluorescence was visualized using a fluorescence microscope (Axio Imager 2_apotome; ZEISS).

Nile red staining of lipid droplets

Parasites were allowed to infect and grow in confluent monolayer HFF grown on coverslips, in the ± ATc conditions for 24 h in 0%/1%/10% FBS ED1 medium. As with IFA, these coverslips were fixed using 2.5% PFA, permeabilized with 0.25% Triton X-100. Thereafter, coverslips were incubated for 1 h with Nile red in 1X PBS before proceeding to DNA staining with Hoechst. The coverslips were mounted onto a glass slide in fluorogel prior to imaging using a fluorescence microscope (Axio Imager 2_apotome; ZEISS). For visualizing Nile red-stained droplets yellow-gold fluorescence (excitation, 450–500 nm; emission, greater than 528 nm) was used on the Axio Imager. Quantification in ± ATc conditions was done by counting the no. of lipid droplets per parasite.

Western blot analysis

Parasites were harvested for Western blot after complete egress from their host. To remove any host cell debris, the parasites were passed through a 3 μm filter, then counted by hemocytometer and solubilized in SDS buffer at equivalent cell densities. An equal amount of protein was separated on a 4%–12% gradient SDS-polyacrylamide (Life Technologies) and transferred to the Nitrocellulose membrane using the XCellII Blot Module (Invitrogen). Primary antibodies anti-HA (Rat, Roche) and anti-TOM40 (Rabbit) [28] were used at a dilution of 1:500 and 1:1000, respectively. Secondary goat anti-mouse and anti-rabbit horse radish peroxidase (HRP) conjugated antibodies (Thermo Scientific) were used at 1:2000. Protein signal was detected by chemiluminescence after membrane staining with Luminata Crescendo Western HRP detection kit (Millipore). The signal strength of the protein was quantified using a BioRad Chemidoc imager (BioRad).

Phenotypic analysis

Plaque assay- The extracellular parasites were harvested after filtration and counted by a hemocytometer. Then approx. 500 parasites were inoculated to confluent HFF flask (25 cm^2). The mutant parasite *Tg*ACS3-ikD was grown for plaque assay in the presence or absence of ATc (0.5 μg ml−1) for 7–10 days. Plaque sizes were visualized by crystal violet staining (30–60 min) after aspiration of culture media, and cells fixation with 100% ethanol (5 min) followed by phosphate-buffered saline (PBS) wash.

Replication assay- The parasites were grown for two days with or without ATc (0.5 μg ml−1), harvested, and filtered. An equal number of parasites were allowed to invade confluent HFF grown on coverslips. Following 2 h of invasion, the coverslips were washed thrice with ED1 (1% FBS containing DMEM), to remove any uninvaded parasites and promote synchronized replication. Anhydrotetracycline (ATc) (0.5 μg ml−1) was added at the outset of the experiment, allowing the treatment for 24 h, alongside control parasites without ATc. These coverslips were then fixed and processed for IFA wherein the parasite number per parasitophorous vacuole was analyzed.

Lipidomic analysis

The parasites were grown for 48 h or until completely extracellular in conditions of ± ATc on the confluent monolayer of HFF in flasks (175 cm^2). For extracellular parasite lipid analyses completely, egressed parasites were collected, and host cells were filtered out with a 3-μm pore size membrane, after which parasites were incubated for 6 h in the respective media conditions 0/1/10% FBS). Parasites were also harvested as the intracellular tachyzoites (1×10^7 cell equivalents per replicate) after syringe filtration with 3-μm pore size membrane. These parasites were metabolically quenched by rapid chilling in a dry ice-ethanol slurry bath and then centrifuged down at 4∘C. The parasite pellet thus obtained was washed with ice-cold PBS thrice, before transferring the final pellet to a microcentrifuge tube. Then total lipids were extracted in chloroform/methanol/water (1:3:1, v/v/v) containing PC (C13:0/C13:0), 10 nmol and C21:0 (10 nmol)

as internal standards for extraction) for 1 h at 4∘C, with periodic sonication. Then polar and apolar metabolites were separated by phase partitioning by adding chloroform and water to give the ratio of Chloroform/Methanol/Water, 2:1:0.8 (v/v/v). For lipid analysis, the organic phase was dried under N_2 gas and dissolved in 1-butanol to obtain 1μl butanol/10^7 parasites.

Total lipid analysis. Total lipid was then added with 1 nmol pentadecanoic acid (C15:0) as internal standard and derivatized to give fatty acid methyl ester (FAME) using trimethylsulfonium hydroxide (TMSH, Machenery Nagel) for total glycerolipid content. Resultant FAMEs were then analyzed by GC-MS as previously described (29, 30). All FAME were identified by comparison of retention time and mass spectra from GC-MS with authentic chemical standards. The concentration of FAMEs was quantified after initial normalization to different internal standards and finally to parasite number.

Phospholipid and neutral lipid analysis. For phospholipid analysis, the total lipid extracted (as mentioned earlier) was separated with 1 nmol PA(C17:0/C17:0) (Avanti Polar lipids) by one-dimensional silica gel high-performance thin layer chromatography (HPTLC, Merck). Total PL, DAG, TAG, Free fatty acids (FFA), and cholesteryl ester (CE) analysis, total lipid fraction was separated by 1D-HPTLC using hexane/diethyl ether/formic acid, 80:20:2 (v/v/v) as solvent system. Thereafter, each lipid spot on the HPTLC plate was scrapped off and lipids were methanolized with 200 μl 0.5 M methanolic HCl in the presence of 1 nmol pentadecanoic acid (C15:0) as internal standard at 85°C for 3 h. The resulting FAMEs were extracted with hexane and finally analyzed by GC-MS (Agilent).

Tracking host-derived fatty acids–(monitoring parasite scavenging capacities). The HFF cells were grown (1 × 10⁸ cell equivalents per replicate) to confluency in the presence of stable isotope U-13C-glucose at a final concentration of 800 μM added to a glucose-free DMEM (10% FBS). These 13C-pre labeled HFF were then infected with *Tg*ACS3-ikD parasites in the presence of normal-glucose-containing DMEM under ± ATc (0.5 μg/ml). The host HFF and parasites were metabolically quenched separately, and their lipid content was quantified by GC-MS as described above. As described previously, the degree of the incorporation of 13C into fatty acids (%carbon incorporation) is determined by the mass isotopomer distribution (MID) of each FAMEs. The total abundance of 13C-labelled fatty acids was analyzed initially for HFF to check the labeling of the metabolites (8). Later, the same was calculated for parasites to confirm the direct uptake of 13C-labelled fatty acids from the host.

Digitonin fractionation. Intracellular tachyzoites were recovered and washed once in PBS. After centrifugation at 1,800 rpm, 10 min at room temperature, parasite concentrations were adjusted exactly at 100 Millions/ml in STE buffer (sucrose 250 mM, Tris-Hcl pH7.4 25 mM, EDTA 1 mM). 100 Million (10⁸) of these parasites were centrifuged and resuspended in 98 μl of ice-cool STEN buffer (STE buffer with NaCl 150 mM, PMSF 0.1 mM). Next, these parasites were warmed at room temperature before adding 2 μl of Digitonin at a concentration of 0.5 mg/ml (DMSO). After 5 s of vortex parasites were incubated for exactly 4 min and then centrifuged for 2 min at 2,000g. a) The pellet fraction was resuspended directly in 200 μl

of Urea buffer 8M. b) The supernatant fraction was precipitated by adding 15 μl of 10% TCA, mixed manually briefly, and incubated 30 min on ice. After centrifugation, pellets were washed in 70% ETOH and then resuspended in 200 μl of Urea buffer 8M. Each fraction (supernatant and pellet) was sonicated for 30 min. Western-blotting: 30 μl of each fraction was mixed with 15 μl of Sample buffer (3x, with beta-mercaptoethanol), denatured 5 min at 95°C.

Statistical analysis for all experiments

The entire graphical data for this study was generated using GraphPad Prism software (version 8). Three biological replicates were used per experiment (n = 3). The error bars are representative of the standard error of mean (SEM) for each study. Statistical significance was determined for each experiment by *t* test using GraphPad Prism. The range of statistical significance was signified as per the *P* value, wherein 0.01–0.05 = *, 0.01–0.001 = **, and <0.001 = ***.

RESULTS

Cellular localization of seven genes encoding putative acyl-CoA synthetase (ACS) enzymes within the *Toxoplasma* genome

To confirm the putative acyl-CoA synthetases (ACS) present in *T. gondii* (22), we conducted a bioinformatic analysis (ToxoDB.org) to search for genes bearing the typical domains defining eukaryotic ACS: the AMP-binding domain as well as the conserved Acyl-CoA synthetase domain Motifs I-V (19). This led to the identification of seven putative ACS potentially expressed during tachyzoite stages (Fig. 1). To further determine their endogenous expression and physiological localization of the seven putative *Tg*ACS, we generated *T. gondii* tachyzoite parasite lines expressing each protein fused to a C-terminal triple haemagglutinin (3×HA) epitope-tag under control of their endogenous promoter (31). Immunofluorescence assays (IFA) using anti-HA antibody revealed that the seven *Tg*ACSs localize to distinct sub-cellular compartments of the parasite (Fig. 1A). *Tg*ACS1, *Tg*ACS6, and *Tg*ACS7 were localized widely within the parasite cytoplasm, mostly as vesicular/punctate patterns. *Tg*ACS2 was predicted and present in a structure reminiscent of the parasite mitochondrion, which is an important eukaryotic metabolic hub for lipid synthesis and catabolism. To precisely confirm the localization of *Tg*ACS2, we conducted confocal microscopy and 3D reconstruction on *Tg*ACS2-iKD-HA with the *T. gondii* mitochondrial outer membrane marker TOM40. These analyses confirmed the close vicinity and the co-localization of *Tg*ACS2 with the parasite mitochondrion (supplemental Fig. S1A, B). Interestingly, the N-terminally tagged *Tg*ACS2-iKD-HA migrated approximately 10 kDa higher than the endogenously C-terminally tagged *Tg*ACS2-HA, with an apparent size of ~103 kDa, correlating its predicted size on ToxoDB (supplemental Fig. S1C). Western blot and IFA analyses

both confirmed the downregulation of *Tg*ACS2-iKD-HA (supplemental Fig. S1day, e) parasite line by anydrotetracycline (ATc) treatment. Complete protein depletion was observed at 24 h and 48 h after ATc treatment. IFA further revealed that the ATc treatment leading to *Tg*ACS2 depletion did not affect the overall morphology of intracellular tachyzoites. The disruption of *Tg*ACS2 had no significant effect on the intracellular development of tachyzoites at any levels of host nutrient (0%, 1% or 10% FBS) as shown by the absence of difference in plaque area also represented graphically (supplemental Fig. S1E, F). *Tg*ACS3 was broadly localized at the cytosol, accumulating around, and avoiding the nuclear area of the parasite. *Tg*ACS4 showed a distinct and interesting peri-nuclear/ER-like localization. Finally, *Tg*ACS5 displayed a cytoplasmic localization, particularly enriched at the basal end of the parasite (Fig. 1). Such specific and diverse localizations suggest non-redundant functions of ACSs within the different endomembrane compartments and cytoplasm of *T. gondii* similarly to the ACSs in other eukaryotes, which have different fatty acid substrate specificities and functions depending on their differential localizations (18, 32, 33).

*Tg*ACS3 is critical for tachyzoite intracellular development, especially in high-host nutrient environments

*Tg*ACS3 (TGGT1_310080) is predicted to be essential for intracellular growth based on its phenotypic score of −2.53 (19), (https://toxodb.org/toxo/app), which reflects its importance for intracellular development in a nutrient-rich environment. We thus decided to focus on the characterization of *Tg*ACS3, as it may play a crucial role in the membrane biogenesis of the rapidly dividing tachyzoite for of *Toxoplasma gondii*. To determine the function and importance of *Tg*ACS3, we generated an inducible knockdown line of *Tg*ACS3 (Fig. 2) by promoter replacement using the Tet-off system in TATi_ΔKu80 background (34, 35) with an additional N-terminal HA-tagging. We confirmed the conditional mutant by PCR (supplemental Fig. S2) The endogenously tagged parasite line was further confirmed by Western blot analysis using an anti-HA antibody (Fig. 2A). The migration of all the *Tg*ACS3-HA was in accordance with their annotated protein sizes on ToxoDB, around 85 kDa. Western blot and IFA analyses both confirmed the downregulation of *Tg*ACS3-iKD-HA parasite line by anhydrotetracycline (ATc) treatment (Fig. 2A, B). Complete protein depletion was observed at 48 h after ATc treatment for *Tg*ACS3 (Fig. 2A). IFA confirmed *Tg*ACS3 is located at the cytosol/perinuclear compartment (Fig. 2B), and seems mainly associated with the organellar fraction in the intracellular tachyzoites, unlike *Tg*ACS1, as suggested by digitonin fractionation approach (supplemental Fig. S3). The disruption of *Tg*ACS3 seems to have a direct deleterious effect on tachyzoite intracellular morphology, especially in
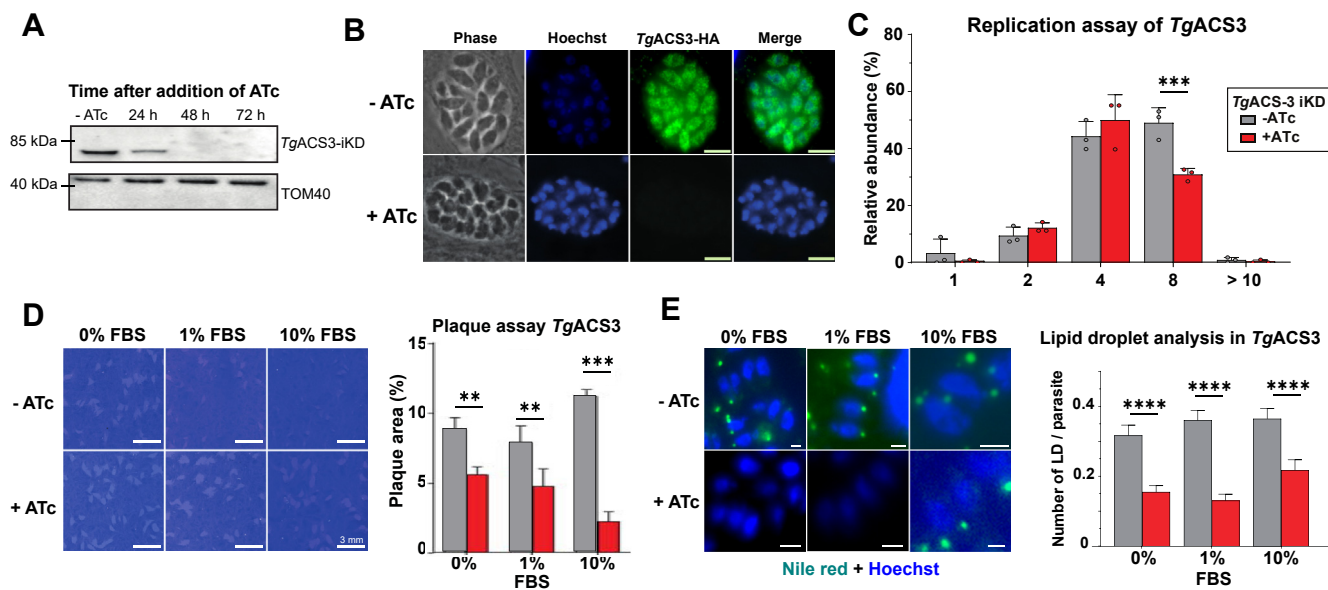

Fig. 2. Cellular characterization of *Tg*ACS3-iKD reveals its critical role in intracellular growth and LD formation. A: Immunoblot analyses revealed downregulation of *Tg*ACS3-iKD (87 kDa) in the presence of anhydrotetracycline (ATc) after 48 h with a TOM40 (40 kDa) loading control. B: *Tg*ACS3 localizes to the cytosol of intracellular parasites with complete loss of signal under ATc treatment (Scale bars = 2 μm). C: A replication assay revealed an increase in vacuoles of 2–4 parasites and a decrease in larger vacuoles (>8 parasites). D: Plaque assay (Scale bars = 3 mm) with statistical analyses showing inhibition of parasite growth when *Tg*ACS3 is degraded at 0%, 1%, and 10% FBS. E: Lipid droplet analyses using Nile red staining (green), showed under *Tg*ACS3 suppression there was a decrease in lipid droplet number per parasite (Scale bars = 2 μm), as confirmed by statistical analyses in the accompanying graph at 0%, 1% and 10% FBS. Error bars indicate standard deviation (SD), Experiments were conducted in triplicates, unpaired *t* test *P* values where 0.01–0.05 = *, 0.01–0.001 = **, <0.001 = ***, and <0.0001 = ****.

large vacuoles (>10 parasites) where parasites appeared round and unhealthy than compared to their usual crescent shape in the presence of *Tg*ACS3 ([Fig. 2](#)B, lower panel: phase). This growth phenotype was confirmed by a replication assay where *Tg*ACS3-depleted parasites had significantly fewer large vacuoles (7–10 parasites) and a significantly higher number of smaller vacuoles (3–6 parasites) ([Fig. 2](#)C), indicating that intracellular division-propagation were significantly impaired in the mutant. We previously showed that wild-type parasites could sense the host's nutritional status, and rewire its metabolic program as well as the host cell's in order to obtain nutrients and lipids to maintain optimal conditions for intracellular survival when the host nutrient content is either too limiting or too rich ([12](#)). Some genes can therefore become more essential under one or another nutritional conditions, that is, limiting or rich. To determine whether *Tg*ACS3 could have a more important role under certain nutritional content, we thus performed plaque assays of *Tg*ACS3 mutant (i.e. typical growth assay conducted for *T. gondii*) in the presence of different host nutritional environments, containing either 0%, 1% and 10% FBS (as to mimic low, regular, and rich host nutrient content, respectively). The disruption of *Tg*ACS3 strongly disrupted parasite growth in all nutrient content. However, this reduced growth phenotype was significantly higher when host nutrient content was higher ([Fig. 2](#)D). When grown in regular culture conditions with 1% FBS, parasites lacking *Tg*ACS3 had significantly smaller and lesser plaques than wild types, although the growth phenotype was significantly lesser than the control ([Fig. 2](#)D). Importantly, when grown in high nutrient environment, at 10% FBS, parasites lacking *Tg*ACS3 displayed a much stronger growth phenotype than at 0% and 1% FBS, with significantly lesser and smaller plaques than in the control ([Fig. 2](#)D). Taken together, this indicates that *Tg*ACS3 is critical for intracellular growth, especially under high host nutrient content, suggesting it may have a role in channeling scavenged FA, as previously reported for *Tg*Lipin ([8](#)).

We recently showed that the bulk of scavenged FA from the host needs to be stored in lipid storages, that is, lipid droplets (LD), to avoid lipotoxic accumulation of free FA (FFA) in the parasite, and to allow the timely mobilization during parasite division ([8](#)). Therefore, we sought to monitor the content of parasite LD in the absence of *Tg*ACS3. Using Nile red, that stain neutral lipid and thus LD, disruption of intracellular *Tg*ACS3 at 0%, 1% and 10% FBS induced a significant reduction in the number of LDs per parasite in all conditions ([Fig. 2](#)E). This suggests that *Tg*ACS3 may play a role in the formation of neutral lipids and storage either directly or indirectly, and further comfort our hypothesis that *Tg*ACS3 could promote the use of host scavenged lipids.

Disruption of *Tg*ACS3 leads to a decrease of TAG levels only in a high host nutrient environment

Our data demonstrates that *Tg*ACS3 has a crucial role in parasite division, overall intracellular tachyzoite development, and utilization of FA for LD biogenesis. To determine its function for parasite lipid homeostasis and/or synthetic capacities, we performed lipidomic analysis on *Tg*ACS3-iKD ± ATc (48 h time point) using GCMS approaches ([8](#)). We first determined the overall FA abundance and composition from the parasite total lipid fraction, which includes all FAs extracted from all parasite glycero(phospho)lipids, neutral lipids, and FFA, under normal host nutrient content, at 1%FBS. Overall, there was a significant difference in the total FA abundance from total parasite lipids in the absence of *Tg*ACS3 (in red, +ATc, **[Fig. 3](#)**A). However, the detailed profile of the total FA composition at 1%FBS showed a significant increase in palmitic acid (C16:0) with a concomitant significant decrease in C20:1 content in the mutant (in red, +ATc, [Fig. 3](#)B). Based on the predicted function of *Tg*ACS3 to metabolically activate FFAs, and the significant reduction of LD upon the disruption of *Tg*ACS3, we further sought to assess the content and profiles of major parasite lipid classes upon *Tg*ACS3 disruption. We thus separated the major lipid classes by HPTLC, namely phospholipids (PL, the major membrane lipids), triacylglycerols (TAG) the main storage lipids found in LD, and FFA, the putative substrates of *Tg*ACS3, which were then all quantified by GCMS analysis. Interestingly, this revealed that FFAs were significantly increasing in the parasite upon *Tg*ACS3 disruption under 1% FBS content ([Fig. 3](#)C). However, disruption of *Tg*ACS3 resulted in no significant change in TAG or PL levels in the parasite in 1% FBS content ([Fig. 3](#)C). Under such low lipid environment (1% FBS), the reduced number of LD per parasite is not correlated with a decrease in TAG level in the absence of *Tg*ACS3. Since TAG levels are unchanged it is possible that, as in mammalian systems, deletion of Perilipins, a protein family found on the surface of LDs, do not affect the amount of TAG but LDs do not assemble, and the lipid is dissolved in membranes ([30](#), [36](#)). Also, this could be due to the ability of *T. gondii* to scavenge FAs and TAG directly from the host, as we know that some phospholipases can recruit FAs and TAGs directly from the host LDs that localizes in the PV of the parasite ([7](#)). Detailed quantification of the FA composition of the FFA fraction revealed a significant decrease in short-chain FAs C14:0 and C16:0 and a significant increase in long-chain FA chains: stearic acid (C18:0) and C22:1 under the depletion of *Tg*ACS3 ([Fig. 3](#)D). These long chain FAs are usually scavenged by the parasite, highlighting the possibility that *Tg*ACS3 could be involved in the activation of FFA coming from the host. Taken together, these data suggest that *Tg*ACS3 disruption causes a significant accumulation of long-chain FFA, suggesting that *Tg*ACS3 likely activates
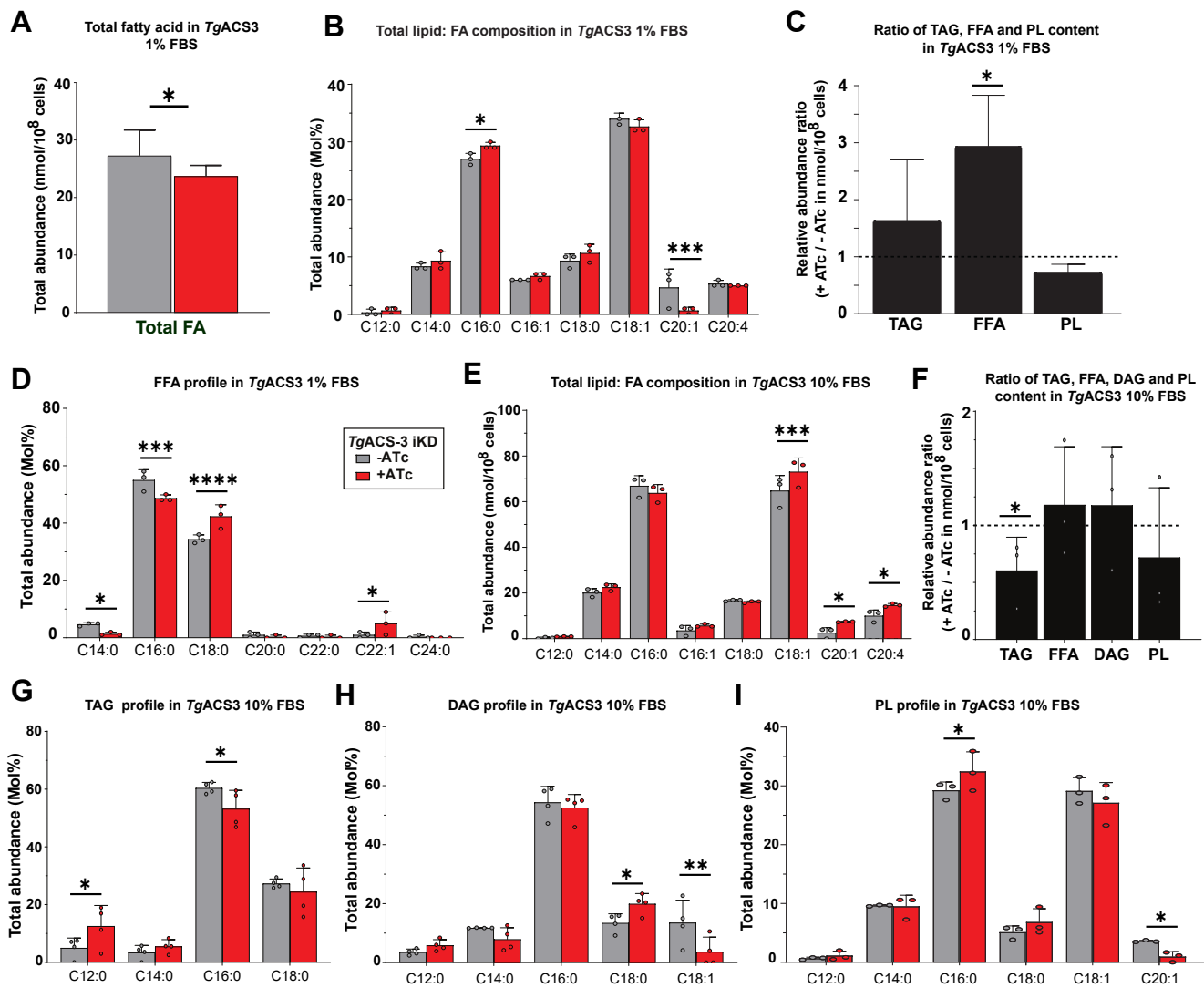
Fig. 3. Lipidomic analyses of *Tg*ACS3-iKD mutant under high and low host nutrient content show its pivotal role for FA activation and for TAG and PL synthesis. A: Under anhydrotetracycline (ATc) treatment (red), the loss of *Tg*ACS3 does not affect the total fatty acid (FA) content of intracellular tachyzoite parasites. B: The FA molecular composition in 1% FBS shows an increase in C16:0 and a decrease C20:1 under the suppression of the protein. C: Relative abundance ratios calculated for TAG, FFA and PL levels without/ with the protein in low level (1% FBS), with D) the molecular compositions of the FFA fraction showing a short chain FA (C14:0, C16:0) and increase in long-chain FA (C18:0, C22:1) under *Tg*ACS3 depletion. E: Under 10% FBS conditions the analyses of the total FA abundance revealed an increase in long-chain FA (C18:1, C20:1, C20:4). F: Relative abundance ratios calculated for TAG, FFA, DAG, and PL levels without/with the protein in high level (10% FBS), with the mol% of the FA composition of (G) TAG, (H) DAG and (I) PL levels. Error bars indicate standard deviation (SD), Experiments were conducted in triplicates, unpaired *t* test *P* values where 0.01–0.05 = *, 0.01–0.001 = **, <0.001 = ***, and <0.0001 = ****.

long-chain FFA to be used by the parasite. Here, in the absence of *Tg*ACS3, long-chain FFA are not activated and thus are accumulating as they are not mobilized. This, in return, might cause a lipotoxic effect on the parasite, correlating with the growth defect phenotype observed at 1% FBS (Fig. 2D).

Since the growth phenotype of *Tg*ACS3-iKD was dramatically increasing in high host nutrient content at 10% FBS, we further investigated the lipidomic profile of parasites lacking *Tg*ACS3 under a high serum and lipid content, at 10% FBS, instead. Total lipid FA composition analyses revealed a further significant

increase in FA chains that are normally scavenged directly from the host: C18:1, C20:1, and C20:4, (Fig. 3E) (8, 12). Detailed quantification of the content from major lipid classes, TAG, DAG, FFA, and PL by 1D-HPTLC and GCMS analysis, revealed a major significant decrease in the relative abundance of TAG levels without *Tg*ACS3 (Fig. 3F). On the other hand, disruption of *Tg*ACS3 at high nutrient content (10%) had no significant effect on the content of DAG and PL. Detailed analyses of the content of each class (Fig. 3G–I) revealed that in these conditions, TAG was significantly lacking C16:0 whereas, PL were significantly accumulating this

FA species (Fig. 3G, I). There was an increase in Cl2:0 and a decrease in Cl6:0 FA chains in the TAG levels when the protein was suppressed (Fig. 3G), suggesting that most of the TAGs are coming directly from the parasite and not scavenged as lipid droplets from the host (8). An increase in the relative abundance of Cl8:0 and decrease of Cl8:1 in DAG levels was also observed (Fig. 3H). On the other hand, there was a general trend of a decrease in unsaturated FAs chains (Cl8:1, C20:1) and a compensating increase of saturated FAs (Cl8:0, Cl6:0) in both lipid classes in the absence of *Tg*ACS3 (Fig. 3H, I). Altogether, these results suggest that *Tg*ACS3 is important for activating long-chain FAs to be used for TAG synthesis, and depends on the nutritional conditions.

*Tg*ACS3 is responsible for channeling the bulk of host-scavenged FA

Based on the lipidomic data showing the major effect of *Tg*ACS3 depletion on long-chain fatty acids (>16:0/18:0), previously shown to be mostly scavenged from the host (8, 12), we further examine the source of FA activated by *Tg*ACS3 within the parasites. We performed a novel flux analysis approach, using U-13C-glucose (Glc) combined to GCMS-lipidomics to monitor and quantify the FA scavenged from the host, that is, the parasite "FA scavengeome" (8). 13C-Glc-pre-labelled host cells were infected with *Tg*ACS3-ikD parasites (+/ATc) in the presence of a normal culture medium, which contains regular 12C-Glc (8). The total lipid content was extracted from the parasites to determine the amount of 13C incorporation to each FA originating from the host. The wild-type *Tg*ACS3-ikD parasites were able to

scavenge FAs from the host, with a significant decrease in host-derived Cl8:1 in the absence of the protein (**Fig. 4**A). Detailed analysis of each FA species shows that there was an overall decrease in FAs scavenged from the host for TAG (Cl6:0, Fig. 4B), DAG (Cl6:0, Fig. 4C) and PL (Cl6:0, Cl8:1, Fig. 4D) in 10% FBS. Interestingly, when we looked at the FFA profile, we observed a significative increase in long-chain FAs Cl6:0 and Cl8:1 scavenged from the host (Fig. 4E). This data suggests that the *Tg*ACS3 majorly acts on long-chain FA scavenged directly from the host, especially in a high host lipid environment balancing between PL synthesis and lipid storage. The increase in host-derived FFA suggests without this protein they cannot be incorporated to form PL and other storage lipids like DAG/TAG.

DISCUSSION

Acyl CoA synthetases catalyze a fundamental and limiting reaction in FA metabolism: the activation of FFA via thioesterification to coenzyme A (CoA). This key reaction allows the fatty acyl-CoA intermediates to participate further in trafficking, assembly into complex lipids, post-translational modification of membrane proteins, and/or the catabolism of FAs via β-oxidation (18). Here, we identified seven putative ACSs expressed in *T. gondii* genome. We focused on *Tg*ACS3 as it was the one with the most dramatic predicted phenotypic scores due to their largely distinct roles in lipid metabolism and nutrient adaptation in other models (nutrient scarcity and excess) and its high predicted phenotypic score (19, 22, 37–40).
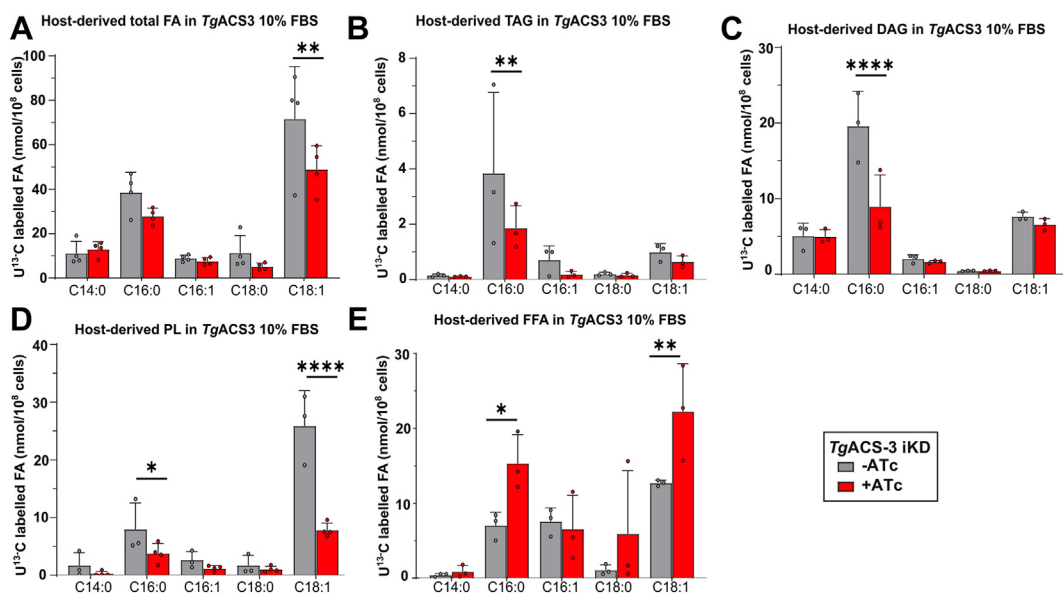
Fig. 4. Lipid flux analyses of host-derived lipids in the *Tg*ACS3-iKD mutant under high host nutrient content. Using 13°C stable isotope-prelabelled host cells, scavenged 13C-lipid profile and abundance channeled into the parasite membranes were quantified by GCMS approach for A: total FA, B: TAG, C: FFA, D: DAG, and E: PL fractions in high nutrient content, that is 10% FBS. Error bars indicate standard deviation (SD), Experiments were conducted in triplicates, unpaired *t* test *P* values where 0.01–0.05 = *, 0.01–0.001 = **, <0.001 = *** and <0.0001 = ****.

The localization of the ACSs could also direct the fate of the acyl-CoAs by allowing the ACSs to interact with different proteins involved in the direct downstream processing. Recent data, including ours, provide evidence for the presence of an active acyl-CoA binding protein-2 (ACBP) that localizes to the mitochondria of the parasite (4, 10). We suggest that *Tg*ACS2 (mitochondrial vicinity) and *Tg*ACBP2 are potentially coherently involved in FA activation and transport within the parasite mitochondria. However, whether they participate in mitochondrial membrane biogenesis is yet to be determined. Eukaryotic TAG biosynthesis occurs as the last step of the glycerol-3-phosphate pathway by the sn-3 acylation of DAG by a diacylglycerol-acyltransferase (DGAT, Fig. 4A) (41, 42). Here we tested the roles of *Tg*ACS3 in this process by comparing the levels of neutral lipids within the reservoir organelles called lipid droplets (LD) by Nile red staining (43). This suggests that *Tg*ACS3 plays a role in the formation of neutral lipids and storage either directly or indirectly.

In metabolically active hepatocyte cells Huh7, ACSL3 has been shown to specifically channel activated FA (esp. C18:1, oleic acid) into phosphatidylcholine. A siRNA-mediated knockdown of ACSL3 decreases oleate incorporation to PC with a concomitant rise in the levels of cellular-free oleic acid (44). Like this study, the measured decrease of the total levels of FA content derived from phospholipids in the *Tg*ACS3-iKD alongside concomitant increase of FFA both corroborate with the functional role of the enzyme (Fig. 2C). We see a drop in TAG levels under depletion of the protein in 10% FBS which is supported by the decrease in LD number per parasite in the absence of *Tg*ACS3 (Fig. 2G). Lipidomic analysis of *Tg*ACS3-iKD + ATc illustrated an upregulation of the normally FASII-derived FAs to compensate for the decrease in host-derived FAs like C20:1 (Fig. 2B). In a high host nutrient environment (10% FBS), we see an increase in the total lipid abundance of even more long-chain unsaturated FAs that are normally host-derived like C18:1, C20:1, and C20:4 (Fig. 2E). This suggests that *Tg*ACS3 probably is a long chain fatty acyl-CoA ligase which thioesterifies long chain FA scavenged from the host rather than the apicoplast-FASII specific short chain FAs (C14:0 and C16:0). This was supported by our 13C-Glc based flux analyses, where we were able to identify whether the increase of FFAs is host-derived (Fig. 3). There was an overall decrease in host-derived FAs for total lipids, which accounted for the decrease in host-derived FAs of TAG, DAG and PLs pools (Fig. 3).

The growth defect for the *Tg*ACS3-iKD was significantly more pronounced in 10% of serum conditions. This observation can be explained by linking it to lipidomic data showing an increase in the FFA content within *Tg*ACS3-iKD (+ATc) and more specifically an increase in host-derived FFAs (Fig. 4). As per its expected function, due to loss of *Tg*ACS3 within the parasite there is a reduction in the metabolic utilization of FA via thioesterification, and instead of equilibrium in lipid storage and synthesis, we see a decrease in PL synthesis and lipid storage. In the presence of lipid-enriched 10% serum, the parasites normally uptake more FAs, however, are unable to balance its utilization due to the absence of an important acyl-CoA synthetase *Tg*ACS3. This led to 'over scavenging' of host FFAs, which seemed to accumulate instead of being used to form PL/DAG or TAGs in the absence of this protein (Fig. 4). It is possible that *Tg*ACS3 could rather be used for activating FAs from LD for parasite β-oxidation. However, this is rather unlikely as the parasite has to store the constantly scavenged FA to LDs (8), and only seems to use β-oxidation in the extracellular stage (22), altogether, more coherent with the phenotype observed in the absence of *Tg*ACS3.

Despite having a negative phenotype score on *Toxoplasma* genome-wide CRISPR-Cas9 screen (19), the measured growth defect of *Tg*ACS3-iKD in normal nutrient conditions at 1% FBS was not as pronounced as predicted. This could be explained by the low lipid content which reduces scavenging, suggesting that *Tg*ACS3 is more likely involved in the activation of FFA coming from the host cell (**Fig. 5**). Moreover, in the presence of a high host nutritional environment (10% FBS), the phenotype of *Tg*ACS3-iKD was more pronounced, correlating with reported phenotype scores. And indeed, under such high lipid content, the parasite has a preference to use host-derived FAs instead of apicoplast-derived FAs, underlying once again the role for *Tg*ACS3 to activate FFA coming from the host, and not those synthesized de novo by the parasite. However, the replication defect demonstrated the importance of *Tg*ACS3 for the parasite intracellular development.

Inflammatory cytokine (TNF-α) elevation in humans, seems to induce the expression of ACSL1, ACSL3, and ACSL5 (44, 45). Increased ACSL3 levels were also accompanied by increased oleoyl-CoA (activated FA C18:0) levels, mirroring our results of increased oleic acid (FFA) when *Tg*ACS3 is absent. The downstream effect of TNF-α increasing ACSL3 levels promoted LD formation in human endothelial cells which may also be the case in *Tg*ACS3 favoring activation of FFA to be used for TAG formation (44). In a recent study, ACSS3 (the short-chain paralogue of ACSL3) was identified as a gene regulating the stability of lipid droplet-associated protein, PLIN3, and causing the reduction of LD deposits in the prostate (46). These studies suggest that ACS3 proteins are critical to LD metabolism and interact with partner proteins to regulate FFA activation and TAG formation.

This work brings insight into the nutrient-dependent role of *Tg*ACS3, as it is different from *Tg*ACS1 and most probably the other ACSs that exist in *T. gondii* parasites (22). In the absence of *Tg*ACS3,
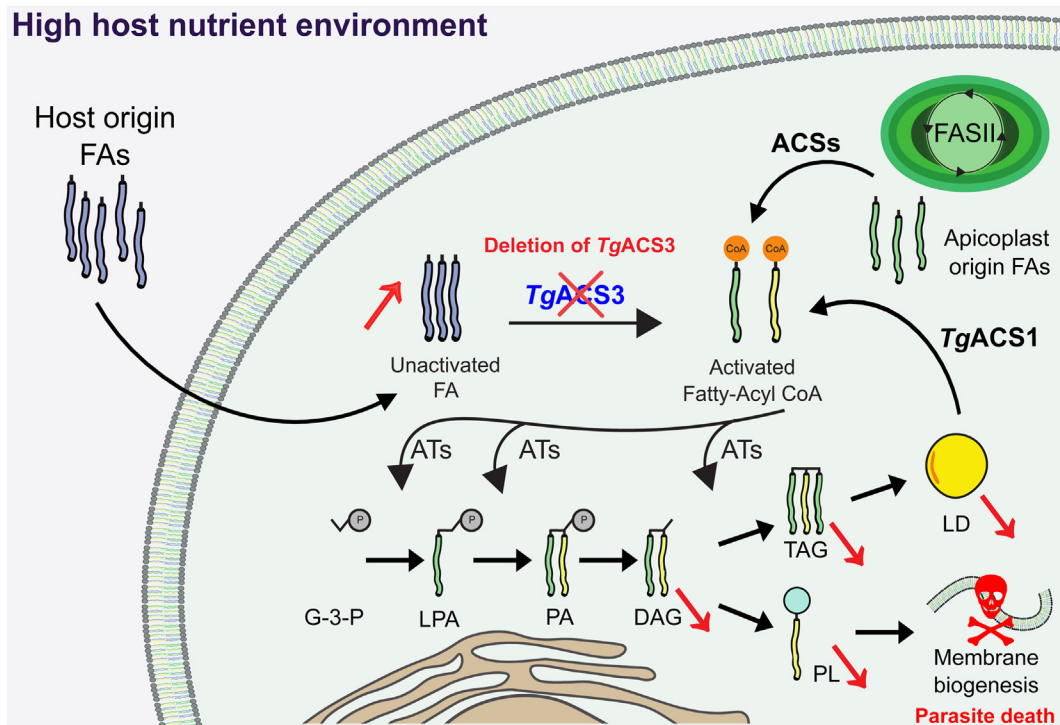
Fig. 5. Model for the proposed roles of *Tg*ACSs in parasite host-adaptation and lipid metabolism. Fatty acids (FA) from the host, extracellular environment, and directly from the parasite are incorporated into the glycerolipid pathway of the parasite. They are esterified onto a glycerol-3-phosphate (G-3-P) by acyltransferase (ATS) like ATS1, ATS2, and AGPAT to form lysophosphatidic acid (LPA) with backbone and phosphatidic acid (PA), respectively. LIPIN is a phosphatase responsible for dephosphorylation of PA to diacylglycerol (DAG) onto which another FA is attached to form triacylglycerol (TAG) by DGAT. FA must be activated to allow for their utilization by ATSs, this is facilitated by acyl-CoA synthetases (ACSs). The downregulation of *Tg*ACS3 leads to effects in intracellular parasites in a high host nutrient environment. There is an "over scavenging" effect that leads to an increase in host-derived and global FFA levels, but this is coupled with a decrease in host-derived TAG, DAG, and phospholipid (PL) levels.

FA coming from the host (represented in blue, Fig. 5) may not be activated, and thus accumulate in the parasite. FAs synthesized de novo in the apicoplast (in green, Fig. 5) and derived from LDs (in yellow, Fig. 5) can be activated by other ACSs (such as *Tg*ACS1, 24). Then, these activated Fatty Acyl CoA enter the glycerolipid pathway to generate DAG and TAG for LD biogenesis or PLs for membrane biogenesis. In the absence of *Tg*ACS3, we observed a decrease in DAG, TAG, and LD as well as a decrease in PLs levels leading to membrane biogenesis defect and parasite death (represented by the red skull, Fig. 5). This protein is important for parasite intracellular development in all conditions, and further accentuated in high host nutrient environment, again illustrating the parasite adapts different metabolic pathways in different conditions, rending them highly plastic (1, 2, 8, 24–26).

Data availability

Most data of this study are present in the current manuscript, or raw lipidomic and fluxomic data are available upon demand to the corresponding authors (Dr Cyrille Botté/Dr Yoshiki Yamaryo Botté; cyrille.botte@univ-grenoble-alpes.fr). 🔓

Author ORCIDs

Serena Shunmugam 🔗 https://orcid.org/0000-0001-6179-3292

Samuel Duley 🔗 https://orcid.org/0000-0002-3419-8057

Christophe-Sébastien Arnold 🔗 https://orcid.org/0000-0002-2392-5837

Yoshiki Yamaryo-Botté 🔗 https://orcid.org/0000-0002-9349-4411

Cyrille Y. Botté 🔗 https://orcid.org/0000-0002-2245-536X

Conflict of interest

The authors declare that they have no conflicts of interest with the contents of this article.

Abbreviations

ACSs, acyl-CoA synthetases; ATc, anhydrotetracycline; CoA, Co-Enzyme A; FAs, fatty acids; *Tg*ACS, ACSs encoded by the genome of T. gondii; TAG, triacylglycerol.

REFERENCES

1. Shunmugam, S., Arnold, C. S., Dass, S., Katris, N. J., and Botté, C. Y. (2022) The flexibility of Apicomplexa parasites in lipid metabolism. *PLoS Pathog.* **18**, e1010313
2. Walsh, D., Katris, N. J., Sheiner, L., and Botté, C. Y. (2022) Toxoplasma metabolic flexibility in different growth conditions. *Trends Parasitol.* **38**, 775–790
3. Ramakrishnan, S., Docampo, M. D., MacRae, J. I., Pujol, F. M., Brooks, C. F., Van Dooren, G. G., *et al.* (2012) Apicoplast and endoplasmic reticulum cooperate in fatty acid biosynthesis in apicomplexan parasite *Toxoplasma gondii. J. Biol. Chem.* **287**, 4957–4971
4. Amiar, S., MacRae, J. I., Callahan, D. L., Dubois, D., van Dooren, G. G., Shears, M. J., *et al.* (2016) Apicoplast-localized lysophosphatidic acid precursor assembly is required for bulk phospholipid synthesis in *Toxoplasma gondii* and relies on an algal/plant-like glycerol 3-phosphate acyltransferase. *PLoS Pathog.* **12**, 1–30
5. Bullen, H. E., Jia, Y., Yamaryo-Botté, Y., Bisio, H., Zhang, O., Jemelin, N. K., *et al.* (2016) Phosphatidic acid-mediated signaling regulates microneme secretion in toxoplasma. *Cell Host Microbe.* **19**, 349–360
6. Bisio, H., Lunghi, M., Brochet, M., and Soldati-Favre, D. (2019) Phosphatidic acid governs natural egress in Toxoplasma gondii via a guanylate cyclase receptor platform. *Nat. Microbiol.* **4**, 420–428
7. Nolan, S. J., Romano, J. D., and Coppens, I. (2017) Host lipid droplets: an important source of lipids salvaged by the intracellular parasite Toxoplasma gondii. *PLoS Pathog.* **13**, 1–38
8. Shunmugam, S., Dass, S., Berry, L., Arnold, C. S., Katris, N. J., Duley, S., *et al.* (2021) Toxoplasma LIPIN is essential in channeling host lipid fluxes through membrane biogenesis and lipid storage. *Nat. Commun.* **12**, 2813
9. Mazumdar, J., and Striepen, B. (2007) Make it or take it: fatty acid metabolism of apicomplexan parasites. *Eukaryot. Cell.* **6**, 1727–1735
10. Fu, Y., Cui, X., Fan, S., Liu, J., Zhang, X., Wu, Y., *et al.* (2018) Comprehensive characterization of toxoplasma acyl coenzyme A-binding protein TgACBP2 and its critical role in parasite cardiolipin metabolism. *mBio.* **9**, e01597-18
11. Pernas, L., Bean, C., Boothroyd, J. C., and Scorrano, L. (2018) Mitochondria restrict growth of the intracellular parasite toxoplasma gondii by limiting its uptake of fatty acids. *Cell Metab.* **27**, 886–897.e4
12. Amiar, S., Katris, N. J., Berry, L., Mcfadden, G. I., Yamaryo-Botté, Y., and Botté, C. Y. (2020) Division and adaptation to host environment of apicomplexan parasites depend on apicoplast lipid metabolic plasticity and host organelle remodeling. *Cell Rep.* **30**, 3778–3792
13. Fu, Y., Cui, X., Liu, J., Zhang, X., Zhang, H., Yang, C., *et al.* (2018) Synergistic roles of acyl-CoA binding protein (ACBP1) and sterol carrier protein 2 (SCP2) in Toxoplasma lipid metabolism. *Cell Microbiol.* **2**, e12970
14. Krishnan, A., Kloehn, J., Lunghi, M., Chiappino-Pepe, A., Waldman, B. S., Nicolas, D., *et al.* (2020) Functional and computational genomics reveal unprecedented flexibility in stage-specific toxoplasma metabolism. *Cell Host Microbe.* **27**, 1–17
15. Liang, X., Cui, J., Yang, X., Xia, N., Li, Y., Zhao, J., *et al.* (2020) Acquisition of exogenous fatty acids renders apicoplast-based biosynthesis dispensable in tachyzoites of Toxoplasma. *J. Biol. Chem.* **295**, 7743–7752
16. Sheokand, P. K., Yamaryo-Botté, Y., Narwal, M., Arnold, C. S., Thakur, V., Islam, M. M., *et al.* (2023) A Plasmodium falciparum lysophospholipase regulates fatty acid acquisition for membrane biogenesis to enable schizogonic asexual division. *Cell Rep.* **42**, 112251
17. Sheokand, P., Narwal, M., Thakur, V., and Mohmmed, A. (2021) GlmS mediated knock-down of a phospholipase expedite alternate pathway to generate phosphocholine required for phosphatidylcholine synthesis in Plasmodium falciparum. *Biochem. J.* **478**, 3429–3444
18. Watkins, P. (2007) Very-long-chain acyl-CoA synthetases. *J Biol. Chem.* **283**, 1773–1777
19. Black, P. N., Dirusso, C. C., Metzger, A. K., and Heimert, T. L. (1992) Cloning, sequencing, and expression of the fudD gene of Escherichia coli encoding acyl coenzyme A synthetase. *J. Biol. Chem.* **267**, 25513–25520
20. Guo, F., Zhang, H., Payne, H. R., and Zhu, G. (2015) Differential gene expression and protein localization of Cryptosporidium parvum fatty acyl-CoA synthetase isoforms. *Article J. Eukaryot. Microbiol.* **63**, 233–246
21. Bethke, L. L., Zilversmit, M., Nielsen, K., Daily, J., Volkman, S. K., Ndiaye, D., *et al.* (2006) Duplication, gene conversion, and genetic diversity in the species-specific acyl-CoA synthetase gene family of Plasmodium falciparum. *Mol. Biochem. Parasitol.* **150**, 10–24
22. Charital, S., Shunmugam, S., Dass, S., Alazzi, A. M., Arnold, C-S., Katris, N. J., *et al.* (2024) The acyl-CoA synthetase TgACS1 allows neutral lipid metabolism and extracellular motility in Toxoplasma gondii through relocation via its peroxisomal targeting sequence (PTS) under low nutrient conditions. *mBio.* **15**, e0042724
23. Bopp, S., Pasaje, C. F. A., Summers, R. L., Magistrado-Coxen, P., Schindler, K. A., Corpas-Lopez, V., *et al.* (2023) Potent acyl-CoA synthetase 10 inhibitors kill Plasmodium falciparum by disrupting triglyceride formation. *Nat. Commun.* **14**, 1455
24. Mancio-Silva, L., Slavic, K., Grilo Ruivo, M. T., Grosso, A. R., Modrzynska, K. K., Vera, I. M., *et al.* (2017) Nutrient sensing modulates malaria parasite virulence. *Nature.* **547**, 213–216
25. Zuzarte-Luís, V., and Mota, M. M. (2018) Cell host & microbe review parasite sensing of host nutrients and environmental cues. *Cell Host Microbe.* **23**, 749–758
26. Sidik, S. M., Huet, D., Ganesan, S. M., Huynh, M. H., Wang, T., Nasamu, A. S., *et al.* (2016) A genome-wide CRISPR screen in toxoplasma identifies essential apicomplexan genes. *Cell.* **166**, 1423–1435.e12
27. Katris, N. J., van Dooren, G. G., McMillan, P. J., Hanssen, E., Tilley, L., and Waller, R. F. (2014) The apical complex provides a regulated gateway for secretion of invasion factors in toxoplasma. *PLoS Pathog.* **10**, e1004074
28. van Dooren, G. G., Stimmler, L. M., and Mcfadden, G. I. (2006) Metabolic maps and functions of the Plasmodium mitochondrion. *FEMS Microbiol. Rev.* **30**, 596–630
29. Dubois, D., Fernandes, S., Amiar, S., Dass, S., Katris, N. J., Botté, C. Y., *et al.* (2018) Toxoplasma gondii acetyl-CoA synthetase is

SASBMB

involved in fatty acid elongation (of long fatty acid chains) during tachyzoite life stages. *J. Lipid Res.* **59**, 994–1004

30. Sztalryd, Carole, and Brasaemle, Dawn L. (2017) The perilipin family of lipid droplet proteins: gatekeepers of intracellular lipolysis. *Biochim. Biophys. Acta Mol. Cell Biol. Lipids.* **1862 (10 Pt B)**, 1221–1232

31. Huynh, M. H., and Carruthers, V. B. (2009) Tagging of endogenous genes in a Toxoplasma gondii strain lacking Ku80. *Eukaryot. Cell.* **8**, 530–539

32. Fulda, M., Shockey, J., Werber, M., Wolter, F. P., and Heinz, E. (2002) Two long-chain acyl-CoA synthetases from Arabidopsis thaliana involved in peroxisomal fatty acid β-oxidation. *Plant J.* **32**, 93–103

33. Schnurr, J. A., Shockey, J. M., de Boer, G. J., and Browse, J. A. (2002) Fatty acid export from the chloroplast. Molecular characterization of a major plastidial acyl-coenzyme A synthetase from arabidopsis. *Plant Physiol.* **129**, 1700–1709

34. Soldati, D., Meissner, M., and Schluter, D. (2002) Role of Toxoplasma gondii myosin A in powering parasite gliding and host cell invasion. *Science.* **298**, 837–840

35. Sheiner, L., Demerly, J. L., Poulsen, N., Beatty, W. L., Lucas, O., Behnke, M. S., *et al.* (2011) A systematic screen to discover and analyze apicoplast proteins identifies a conserved and essential protein import factor. *PLoS Pathog.* **7**, e1002392

36. Griseti, E., Bello, A. A., Bieth, E., Sabbagh, B., Iacovoni, J. S., Bigay, J., *et al.* (2024) Molecular mechanisms of perilipin protein function in lipid droplet metabolism. *FEBS Lett.* **598**, 1170–1198

37. Lopes-Marques, M., Machado, A. M., Ruivo, R., Fonseca, E., Carvalho, E., Filipe, L., *et al.* (2018) Expansion, retention and loss in the Acyl-CoA synthetase 'Bubblegum' (Acsbg) gene family in vertebrate history. *Gene.* **664**, 111–118

38. Poppelreuther, M., Rudolph, B., Du, C., Großmann, R., Becker, M., Thiele, C., *et al.* (2012) The N-terminal region of acyl-CoA synthetase 3 is essential for both the localization on lipid droplets and the function in fatty acid uptake. *J. Lipid Res.* **53**, 888–900

39. Pei, Z., Oey, N. A., Zuidervaart, M. M., Jia, Z., Li, Y., Steinberg, S. J., *et al.* (2003) The Acyl-CoA synthetase 'bubblegum' (lipidosin): further characterization and role in neuronal fatty acid β-oxidation. *J. Biol. Chem.* **278**, 47070–47078

40. Ellis, J. M., Frahm, J. L., Li, L. O., and Coleman, R. A. (2010) Acyl-coenzyme A synthetases in metabolic control. *Curr. Opin. Lipidol.* **21**, 212–217

41. Nolan, S. J., Romano, J. D., Kline, J. T., and Coppens, I. (2018) Novel approaches to kill toxoplasma gondii by exploiting the uncontrolled uptake of unsaturated fatty acids and vulnerability to lipid storage inhibition of the parasite. *Antimicrob. Agents Chemother.* **62**, e00347-18

42. Coppens, I. (2013) Targeting lipid biosynthesis and salvage in apicomplexan parasites for improved chemotherapies. *Nat. Rev. Microbiol.* **11**, 823–835

43. Greenspan, P., Mayer, E. P., and Fowler, S. D. (1985) Nile red: a selective fluorescent stain for intracellular lipid droplets. *J. Cell Biol.* **100**, 965–973

44. Yao, H., and Ye, J. (2008) Long chain acyl-CoA synthetase 3-mediated phosphatidylcholine synthesis is required for assembly of very low density lipoproteins in human hepatoma Huh7 cells. *J. Biol. Chem.* **283**, 849–854

45. Jung, H. S., Shimizu-Albergine, M., Shen, X., Kramer, F., Shao, D., Vivekanandan-Giri, A., *et al.* (2020) TNF-α induces acyl-CoA synthetase 3 to promote lipid droplet formation in human endothelial cells. *J. Lipid Res.* **61**, 33–44

46. Zhou, L., Song, Z., Hu, J., Liu, L., Hou, Y., Zhang, X., *et al.* (2021) ACSS3 represses prostate cancer progression through downregulating lipid droplet-associated protein PLIN3. *Theranostics.* **11**, 841–860